Lysosomal storage of oligosaccharide and glycosphingolipid in imino sugar treated cells

Stephanie D. Boomkamp · J. S. Shane Rountree ·
David C. A. Neville · Raymond A. Dwek ·
George W. J. Fleet · Terry D. Butters

Abstract Sandhoff and Tay-Sachs disease are autosomal recessive GM2 gangliosidoses where a deficiency of lysosomal β-hexosaminidase results in storage of glycoconjugates. Imino sugar (2-acetamido-1,4-imino-1,2,4-trideoxy-L-arabinitol) inhibition of β-hexosaminidase in murine RAW264.7 macrophage-like cells led to lysosomal storage of glycoconjugates that were characterised structurally using fluorescence labelling of the free or glycolipid-derived oligosaccharides followed by HPLC and mass spectrometry. Stored glycoconjugates were confirmed as containing non-reducing GlcNAc or GalNAc residues resulting from the incomplete degradation of N-linked glycoprotein oligosaccharide and glycolipids, respectively. When substrate reduction therapeutics N-butyl-deoxynojirimycin (NB-DNJ) or N-butyldeoxygalactonojirimy-cin (NB-DGJ) were applied to the storage phenotype cells, an increase in glucosylated and galactosylated oligosaccharide species was observed due to endoplasmic reticulum α-glucosidases and lysosomal β-galactosidase inhibition, respectively. Hexosaminidase inhibition triggered a tightly regulated cytokine-mediated inflammatory response that was normalised using imino sugars NB-DNJ and NB-DGJ, which restored the GM2 ganglioside storage burden but failed to reduce the levels of GA2 glycolipid or glycoprotein-derived N-linked oligosaccharides. Using a chemically induced gangliosidosis phenotype that can be modulated with substrate lowering drugs, the critical role of GM2 ganglioside in the progression of inflammatory disease is also demonstrated.

Keywords Gangliosidoses · Hexosaminidase inhibition · Fluorescence labelling · HPLC analysis

S. D. Boomkamp · J. S. S. Rountree · D. C. A. Neville ·
R. A. Dwek · T. D. Butters (✉)
Oxford Glycobiology Institute, Department of Biochemistry,
University of Oxford, South Parks Road,
Oxford OX1 3QU, UK
e-mail: terry.butters@bioch.ox.ac.uk

J. S. S. Rountree · G. W. J. Fleet
Chemistry Research Laboratory, University of Oxford,
Mansfield Road,
Oxford OX1 3TA, UK

Abbreviations

ER	endoplasmic reticulum
ERAD	endoplasmic reticulum associated degradation
GSL	glycosphingolipid
GM2	II^3-α-N-acetylneuraminylgangliotriglycosylcera-mide
GA2	gangliotriglycosylceramide
GlcNAc	N-acetylglucosamine
GalNAc	N-acetylgalactosamine
Hex	hexosaminidase
IL	interleukin
LPS	lipopolysaccharide
MIP-1α	macrophage inflammatory protein-1α
NB-DNJ	N-butyldeoxynojirimycin
NB-DGJ	N-butyldeoxygalactonojirimycin
OS	glycoprotein-derived oligosaccharide(s)
SRT	substrate reduction therapy
TGF-β1	transforming growth factor-β1
TNF-α	tumour necrosis factor-α

Introduction

The GM2 gangliosidoses are a group of lysosomal storage disorders that include Tay-Sachs disease, a deficiency in the α subunit of β-hexosaminidase A (αβ) and Sandhoff disease, caused by a deficiency in the β-subunit in β-hexosaminidase A (αβ) and β-hexosaminidase B (ββ). ß-Hexosaminidase hydrolyses β-glycosidic links of *N*-acetylhexosamine-terminating glycolipids such as GM2 ganglioside and its asialo-derivative GA2, and failure to do so results in progressive accumulation of these glycosphingolipids (GSL), primarily in neuronal lysosomes. Besides GSL accumulation, the levels of N-linked glycoprotein-derived free oligosaccharides (OS) containing *N*-acetylglucosamine (GlcNAc) termini are elevated in Sandhoff disease [1, 2].

It is unclear how the progressive disease pathology is substantiated. *N*-Acetylhexosamine terminating GSL and OS that accumulate in Sandhoff disease mice may contribute to, or cause, disease pathology by triggering an inflammatory response [3]. Macrophage-inflammatory protein-1α (MIP-1α), tumour necrosis factor-α (TNF-α), MHC class II, nitric oxide, interleukin-1β (IL-1β) and transforming growth factor-β1 (TGF-β1) have all been implicated in the disease progression [4–6].

Effective treatment of the neurodegenerative lysosomal storage diseases (LSD), including GM2 gangliosidosis, remains to be found. The existing bone marrow transplantation and enzyme replacement therapy are limited because of inaccessibility imposed by the blood-brain barrier [7]. In contrast to the majority of current therapies, substrate reduction therapy (SRT) is a generic strategy, aimed at depleting GSL biosynthesis *via* inhibition of key enzyme ceramide-specific glucosyltransferase by administration of *N*-alkylated imino sugars, *e.g. N*-butyldeoxynojirimycin (*N*B-DNJ) [8, 9] or *N*-butyldeoxygalactonojirimycin (*N*B-DGJ) [10]. However, the glucose analogue, *N*B-DNJ, is also an inhibitor of intestinal and endoplasmic reticulum (ER) α-glucosidases, leading to unwanted but manageable side-effects in man. *N*B-DGJ is a moderate inhibitor of β-galactosidases, but, in contrast to *N*B-DNJ, appears to elicit reduced side-effects in mouse [11–13]. The effects of these SRT imino sugars on accumulated free *N*-linked oligosaccharide levels, which may contribute to the disease severity in lysosomal storage disorders with affected glycoprotein degradation [3], have not been reported previously. In this paper we have determined the structures of the stored GSL and GlcNAc-terminating OS using HPLC and mass spectrometric techniques in a chemically induced *in vitro* cellular model. By reducing GSL storage levels following treatment with *N*-alkylated imino sugars, the effects of protein-derived oligosaccharide accumulation on cytokine expression were evaluated to reveal the glycoconjugate(s) responsible for the progressive inflammation-led pathology in the GM2 gangliosidoses.

Experimental

Reagents Murine RAW264.7 cell line was purchased from the European Collection of Animal Cell Cultures (Porton Down, UK). Media and PBS were from Invitrogen (Paisley, UK). β-Hexosaminidase inhibitor SR1 (2-acetamido-1,4-imino-1,2,4-trideoxy-L-arabinitol) was synthesised as described previously [14]. Ceramide glycanase from *Hirudu medicinalis* and ß-hexosaminidase and α-mannosidase from jack bean meal were purified in-house. Anthranilic acid (2-AA), sodium cyanoborohydride, p-nitrophenyl-β-D-*N*-acetylglucosamine (PNP-GlcNAc), p-nitrophenyl-β-D-*N*-acetylgalactosamine (PNP-GalNAc), BSA and bicinchoninic acid (BCA) protein-detection kit were obtained from Sigma (Gillingham, UK). HPLC-grade acetonitrile (Far UV, gradient compatible) was from Fisher (Loughborough, UK). Cytokine expression arrays were from RayBiotech (Norcross, USA) and the TGF-β1, MIP-1α and TNF-α ELISA Quantikine kits and intracellular caspase detection kit from R&D Systems (Minneapolis, USA). Enzymes β-hexosaminidase, recombinant ß-*N*-acetylglucosaminidase pGXSTrH17 and α-mannosidase were purified in-house. β-Galactosidase was from Prozyme (San Leandro, USA). *N*B-DNJ and *N*B-DGJ were provided by Celltech (Slough, UK).

Cell culture Murine RAW264.7 cells were cultured in suspension in RPMI1640 medium supplemented with 10% FCS, 1 mM L-glutamine and 1% (v/v) of a stock solution containing 100 U/mL penicillin and 100 μg/mL streptomycin. For the cytokine studies, DMEM (high glucose) containing 2% FCS and 1% (v/v) of the stock solution of penicillin/streptomycin was used. Following culture to confluence for the period indicated, the cells, and/or the respective supernatants, were centrifuged at 1,000 g for 5 min, and washed twice with PBS. The cell pellets were stored at -20°C until use.

Enzyme kinetics The inhibitory potency of SR1 was evaluated by incubating RAW cell homogenates with either 1 mM PNP-GlcNAc or PNP-GalNAc in the presence of various concentrations of inhibitor in 100 mM citrate-phosphate buffer, pH 4.0, at 37°C for 30 min. The reaction was stopped by addition of 0.5 M Na_2CO_3 and the absorbance at 400 nm was measured.

GSL extraction Cell pellets were dounce homogenized in water, followed by GSL extraction, according to a modified Svennerholm method [15], labelling with 2-anthranilic acid (2-AA) and analysis by normal phase-HPLC (NP-HPLC) [15].

OS extraction A fraction of the homogenate was passed through a mixed-bed ion-exchange column [16], followed by labelling with 2-AA and purification through a Spe-ed amide-2 column, prior to NP-HPLC analysis [15].

Carbohydrate analysis by NP-HPLC Purified 2-AA labelled saccharides derived from glycoproteins or GSL were separated by NP-HPLC using a 4.6×250 mm TSKgel Amide-80 column (Anachem, Luton, UK) [15]. Peak areas, measured using Waters Empower software and converted into molar amounts using an experimentally-derived conversion factor (*i.e.* using 2-AA labelling, comparing a standard oligosaccharide of known concentration and measurement of the peak area following HPLC separation), were normalised to protein amount, as measured by a modified BCA assay with BSA as a standard [15].

Structural characterisation of OS species Purified 2-AA GlcNAc-terminating oligosaccharides were further analysed by matrix-assisted laser desorption/ionisation time-of-flight (MALDI-TOF) mass spectrometry using a Micromass TOF-Spec 2E mass spectrometer, in reflectron mode [17]. Nano-electrospray MS was performed on 2-aminobenzamide (2-AB) labelled OS (dried sample was suspended in 0.35 M 2-AB, 1 M sodium cyanoborohydride in water: acetic acid:DMSO (10:30:70, v/v), incubated at 65°C for 2 h, prior to purification through a Spe-ed amide-2 column) with a Waters-Micromass quadrupole-time-of-flight Ultima Global instrument [18].

Enzymatic determination of individual GlcNAc- and galactose-terminating OS species, separated following NP-HPLC, were subjected to digestion with ß-hexosaminidase or β-galactosidase at 50 U/ml at 37°C overnight to completely remove terminal *N*-acetylhexosamine or galactose residues, respectively. Recombinant *Streptococcus pneumoniae* ß-*N*-acetylglucosaminidase pGeXSTrH17 (1.5 U/mL in 50 mM citric acid/sodium phosphate buffer, pH 5.0, containing 1 mg/mL BSA) was used to selectively remove terminal ß1-2 linked GlcNAc residues [19]. The oligosaccharide products were obtained after centrifugation through a 10,000 Da molecular weight cut-off filter (pre-washed with 250 µL water) at 7,000 g for 45 min at room temperature (25°C), to remove proteins prior to NP-HPLC analysis.

Inflammation/apoptosis studies RAW cells were grown in the presence or absence of 50 µM SR1 for up to 30 days. Cells or their respective media were acquired every 5 days. The obtained supernatant was used for cytokine expression analysis according to the manufacturer's instructions, and the amount of cytokine (in pmol) normalised to cellular protein, as determined by BCA assay.

Cell culture media were subjected to cytokine expression assays and DuoSet MIP-1α, TNF-α, TGF-ß1 sandwich

ELISA's (performed according to the manufacturer's instructions). For LPS studies, RAW cells were stimulated with 1 µg/mL LPS for 16 h following which expression assays and ELISAs were performed. Intracellular caspase was measured using flow cytometry following incubation with a cell-permeable, fluorescein isothiocyanate (FITC) conjugated pan-caspase inhibitor (ApoStat), according to the manufacturer's instructions.
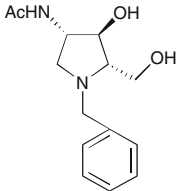
Statistical analysis All experiments were performed with a minimum of three times, using triplicates where possible. Mean±SEM are shown.

Results

SR1 causes accumulation of N-acetylhexosamine terminating GSL and OS in RAW cells SR1 is a novel pyrrolidine imino sugar that stereochemically resembles *N*-acetylhexosamine [14]. In murine RAW264.7 macrophage-like cell extracts, this compound inhibited β-hexosaminidase activity at low micromolar concentrations (Table 1) in a predominantly non-competitive manner using artificial substrates, as determined by Lineweaver-Burk plots (data not shown), consistent with the inhibition of other mammalian and plant-derived hexosaminidases [20]. SR1 also differentially enhances the activity of mutant β-hexosaminidase A and B in cells derived from a Tay-Sachs patient, indicative of an additional, chemical chaperone property at non-inhibitory concentrations [20].

This potent β-hexosaminidase inhibitor caused GM2 and GA2 glycolipid levels to accumulate to 4- and 28 fold that of control levels, respectively, in RAW cells (Fig. 1a), in a time- and concentration-dependent manner (Fig. 2a). At 10 µM SR1, maximal GM2 accumulation was reached, whereas GA2 continued to accumulate with inhibitor concentration. The discrepancy in extent of elevation between the two GSL species is thought to be due to the presence of a mouse-specific sialidase that can convert GM2 to GA2 [21].

Table 1 Inhibition of ß-hexosaminidase. The IC_{50} and Ki values were determined by measuring ß-hexosaminidase activity in RAW264.7 cell homogenates in the presence of SR1 using p-nitrophenyl-GlcNAc and p-nitrophenyl-GalNAc as substrates (mean±SEM)

SR1	PNP-substrate	IC_{50} (µM)	Ki (µM)
	GlcNAc	1.05±0.1	0.94±0.1
	GalNAc	2.89±0.4	0.91±0.1

Fig. 1 Effects of β-hexosaminidase inhibitor SR1 in RAW264.7 cells. Cells were grown in the absence (Control) or presence (+SR1) of 50 μM SR1 for 30 days before analysing **a** GSL and **b** OS by NP-HPLC. The numbered OS species correspond to those in Table 2; 1–3, $GlcNAc_1Man_2GlcNAc_1$ isomers; 4, $GlcNAc_2Man_2Glc$-NAc_1; 5, $Man_4GlcNAc_1$; 6–7, $GlcNAc_2Man_3GlcNAc_1$ isomers; 8, $GlcNAc_3Man_3Glc$-NAc_1; 9, $Man_5GlcNAc_1$; 10, $GlcNAc_4Man_3GlcNAc_1$. Representative profiles from at least three experiments are shown
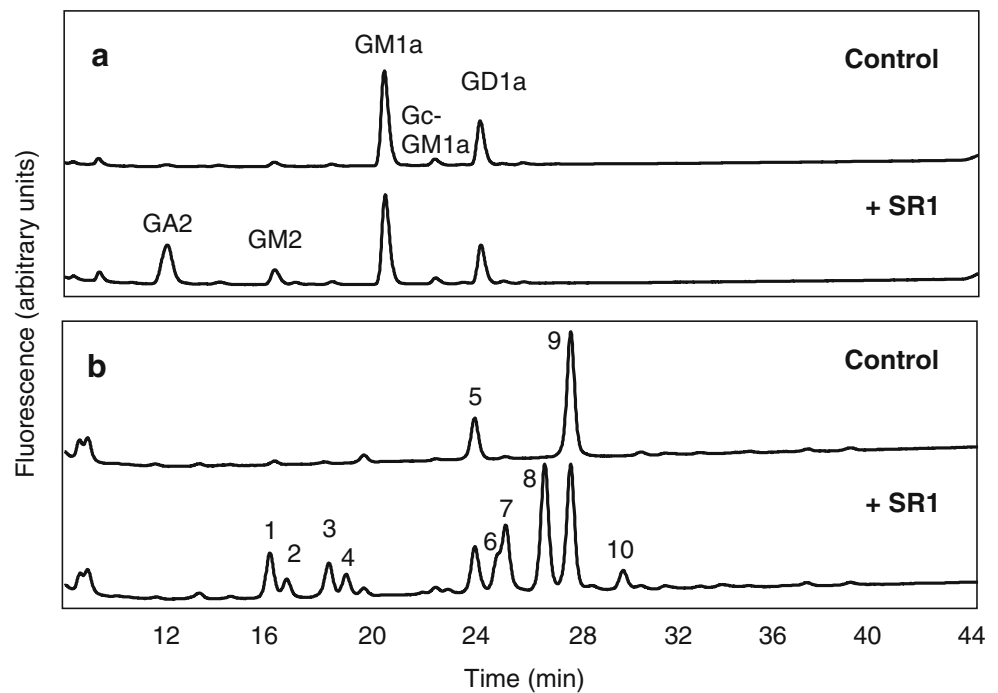

The composition of *N*-linked glycoprotein-derived oligosaccharides (OS) also changed following SR1 treatment. Whereas the levels of control OS (Fig. 1b), products of ER-associated degradation, including that of oligomannose species $Man_4GlcNAc_1$ and $Man_5GclNAc_1$ (structures numbered 5 and 9, respectively), remained constant, SR1 induced storage of GlcNAc-terminating OS (Fig. 1b and 2b). These OS were characterised structurally using enzyme digestion, HLPC and mass spectrometry, as shown in Table 2 and included bi-, tri- and tetra-antennary GlcNAc-terminating species.

Further studies using density gradient fractionation demonstrated that glycolipids GM2 and GA2 and GlcNAc-terminating protein-derived OS were primarily stored in the lysosome (results not shown).

Cytokine expression correlates with glycoconjugate storage
Whereas intracellular changes in cytokine expression remained
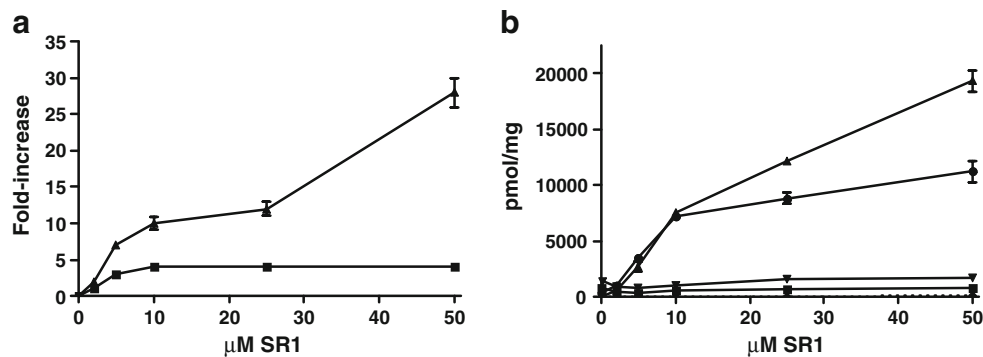
Fig. 2 Effects of SR1 on GSL and OS levels. RAW cells were grown in the presence of up to 50 μM SR1, in triplicate, for 4 weeks followed by **a** extraction of GSL, cleavage of oligosaccharides by ceramide glycanase, and labelling of the released saccharides with 2-AA and analysis by NP-HPLC. GSL species were determined based upon their glucose units (GU), using dextran and a GSL standard an external standard, in addition to acid hydrolysis as described in the experimental procedure. Dose-dependence increase in GM2 (■) and GA2 (▲) levels in SR1-treated RAW cells compared to control cells is illustrated. Three experiments were performed to determine mean ±SEM values. **b** Following extraction of neutral OS, obtained from RAW cells cultured in various concentrations of SR1 for 30 days, mixed bed ion-exchange, labelling with 2-AA and analysis by NP-HPLC was performed. OS species were characterised based on their glucose units, using dextran as an external standard, and mass spectrometry and various enzyme digests using β-hexosaminidase, α-mannosidase and pGEx17 (Table 2). The GlcNAc-terminating OS levels, standardised to protein (pmol/mg) in SR1-treated RAW cells, are shown from three experiments (mean±SEM). The structures were separated as described in Fig 1, as shown in Table 2. $GlcNAc_{1-2}Man_2GlcNAc_1$ OS peaks 1–4 (●); $Man_4GlcNAc_1$, OS peak 5 (■); $GlcNAc_{2-4}Man_3GlcNAc_1$, OS peaks 6–8 and10 (▲); $Man_5GlcNAc_1$, OS peak 9 (▼), $Glc_1Man_5GlcNAc_1$, OS peak b, Fig 3b (–◆–)

Table 2 Structural Characterisation of Oligosaccharide (OS) accumulating in RAW246.7 cells following inhibitor treatment. Oligosaccharides from SR1 treated cells were isolated and separated by NP-HPLC as described and annotated in Fig 1b. Individual species were collected from the chromatography eluate and further characterised by mass spectrometry (m/z) and ß-hexosaminidase, α-mannosidase and linkage specific ß-hexosaminidase (pGex17) digestion. The elution values (in glucose units, GU) are shown before and after enzyme treatment. The OS species containing hexose (H), mannose (Man, M) and N-acetylhexosamine (GlcNAc, N) residues have the proposed structure indicated

No.	m/z	GU	GU β-hex	GU α-man	GU pGex17	OS species	Proposed structure
1	868.3	3.33	2.85	-	3.35, 2.85	H_2N_2	Manβ4GlcNAc-2AA / Manα3 | GlcNAcß4
2	868.3	3.44	2.85	-	2.85, 3.35	H_2N_2	Manβ4GlcNAc-2AA / GlcNAcß2Manα3
3	868.3	3.75	3.06	-	3.08, 3.75	H_2N_2	GlcNAcß2Manα6 \ Manβ4GlcNAc-2AA
4	1071.4	3.88	2.85	-	3.35, 2.86, 3.07	H_2N_3	Manβ4GlcNAc-2AA / GlcNAcß2Manα3 | GlcNAcß4
5*	989.4	4.93	-	2.02	-	M_4N_1	Manα6 \ Manβ4GlcNAc-2AA / Manα3 | Manα2
6	1233.5	5.16	4.02	-	4.62, 4.04	H_3N_3	Manα6 \ Manβ4GlcNAc-2AA / GlcNAcß2Manα3 | GlcNAcß4
7	1233.5	5.22	4.02	-	4.04, 4.62	H_3N_3	GlcNAcß2Manα6 \ Manβ4GlcNAc-2AA / GlcNAcß2Manα3
8	1436.6	5.60	4.02	-	4.62, 4.04	H_3N_4	GlcNAcß2Manα6 \ Manβ4GlcNAc-2AA / GlcNAcß2Manα3 | GlcNAcß4
9*	1151.5	5.85	-	2.02	-	M_5N_1	Manα6 \ Manβ4GlcNAc-2AA / Manα3 | Manα2 | Manα2
10	1639.7	6.41	4.02	-	5.85, 4.63, 4.04	H_3N_5	GlcNAcß6 | GlcNAcß2Manα6 \ Manβ4GlcNAc-2AA / GlcNAcß2Manα3 | GlcNAcß4

[a] present in control cells. pGeXSTrH17 β-hexosaminidase digestion resulted in more than one product and the relative GU values are shown in order of highest abundancy

minimal following SR1 treatment, a dramatic increase in the levels of various secreted pro-inflammatory cytokines including macrophage inflammatory protein-1α (MIP-1α), MIP-1γ, TNF-α, eotaxin-2, CXCL16, interleukins (IL-1α, IL-1β, IL-12p70, IL-4, IL-9), and inflammation-induced apoptosis mediator soluble tumour necrosis factor receptor (sTNF R) I and II, was observed (Supplementary Fig. 1).

Changes in levels of MIP-1α and TNF-α have been implicated in Sandhoff disease [4], consistent with the findings presented here, and are mediated by immunosuppressive transforming growth factor-β1 (TGF-β1) [22]. Consequently, the expression of these cytokines was analysed using quantitative enzyme linked immunosorbent assays (ELISA's). Pro-inflammatory cytokines MIP-1α, TNF-α and mediator transforming growth factor-β1 (TGF-β1) were elevated up to three- or four-fold upon treatment with the β-hexosaminidase inhibitor, in a time-dependent manner (Supplementary Fig. 2A). Interestingly, intracellular caspase levels measured by flow cytometry did not change during SR1 treatment, suggesting SR1 did not cause caspase-dependent apoptosis (Supplementary Fig. 2B).

To determine if SR1-treated RAW cells, challenged by the lysosomal storage, remained capable of mediating their cytokine expression, possibly via immunosuppressive TGF-β1, cells were treated with lipopolysaccharide (LPS). Following LPS addition to non-inhibitor treated RAW cells an elevation in levels of eotaxin-2, interferon-γ (IFN-γ) and IL-4 was observed (Supplementary Fig. 1). By contrast, in SR1-treated cells, the levels of interleukin-6 (IL-6), regulated upon activation, normal T-cell expressed and secreted (RANTES), TNF-α, MIP-1α and MIP-2 were significantly elevated following LPS-treatment. The levels of TGF-β1 were not affected however, in contrast to a 78 and 5-fold increase in TNF-α and MIP-1α expression, respectively (data not shown). This suggests that TGF-β1 was incapable of mediating the inflammatory response and LPS further challenged β-hexosaminidase inhibited cells. However, apoptosis measured by caspase release was not observed (data not shown), suggesting that LPS induced a non-caspase dependent inflammatory response.

N-alkylated imino sugars affect GSL and OS storage levels Treatment with the GSL biosynthesis inhibitors NB-DNJ or NB-DGJ, at concentrations between 5 μM and 50 μM, resulted in restoration of GM2 ganglioside to control levels. However, GA2 was still five-fold that of SR1-untreated cells when treated with 500 μM of either imino sugar (Fig. 3a). The failure of the imino sugars to restore the GA2 storage burden is in agreement with recent findings in mouse models for Sandhoff disease [23]. As expected from the mechanism of action of these imino sugars, the levels of other GSL, for example GM1, were reduced following treatment (Fig 3a).

Both N-alkylated imino sugars affected the oligosaccharide composition in SR1-treated RAW cells by inhibiting different metabolic pathways that are additional to the effects on GSL biosynthesis. Following NB-DNJ treatment a substantial increase in OS species, designated by peak numbers a-f, was observed (Fig. 3b). These OS were characterized structurally as described previously [16], and included mono-, di- and tri-glucosylated $Man_4GlcNAc_1$ and mono-, di- and tri-glucosylated $Man_5GlcNAc_1$ species, ultimately lowering the oligomannose $Man_{4-5}GlcNAc_1$ levels (Fig. 3d). These data confirmed that the generation of glucosylated OS in NB-DNJ treated cells was a consequence of α-glucosidase I and II inhibition [11, 16].

Treatment with the galactose analogue, NB-DGJ, however, resulted in a substantial increase in galactosylated OS species due to lysosomal β-galactosidase inhibition, not previously reported. The galactose-containing OS were structurally characterised following enzyme digestions and HPLC analysis (Fig 3c and Table 3). These structures were based on the GlcNAc-terminating OS, stored as a consequence of β-hexosaminidase inhibition, but capped with one or more galactose residue(s). The overall levels of OS present in SR1-treated RAW cells were not affected however (Fig. 3d), and the absence of an increase in glucosylated OS supported the finding that the galactose analogue has no effect on glucosidase-mediated glycoprotein folding, in contrast to NB-DNJ [10].

As a consequence of α-glucosidase or β-galactosidase inhibition, the total levels of GlcNAc-terminating OS in SR1-treated cells changed. At 5 μM NB-DNJ or NB-DGJ these levels were increased to 150% compared to that in cells treated with SR1 alone (Fig. 3d). Following treatment with 500 μM NB-DNJ or NB-DGJ however, the total levels of GlcNAc-terminating OS were reduced by 30% or 60%, respectively (Fig. 3d).

N-alkylated imino sugars restore inflammatory response The semi-quantitative cytokine expression studies show a time-dependent effect of NB-DNJ and NB-DGJ on the inflammatory response. Treatment with 5 μM imino sugar for 7 days did not ameliorate the cytokine expression significantly whereas long-term treatment, for 30 days, resulted in complete resolution of the cytokine-mediated response (Supplementary Fig. 3). Interestingly, following 7 days treatment with 5 μM imino sugar the GM2 storage levels were still two-fold that of control, whereas after 30 days GM2 storage was not detected (data not shown).

NB-DNJ (Fig. 4a) at a concentration of 5 μM caused a rapid decline in all MIP-1α, TNF-α and TGF-β1 cytokine levels to amounts below those in control RAW cells (Fig 4c). However, when higher concentrations of this glucose analogue were administered to control or SR1-treated RAW cells, the levels rapidly increased to levels
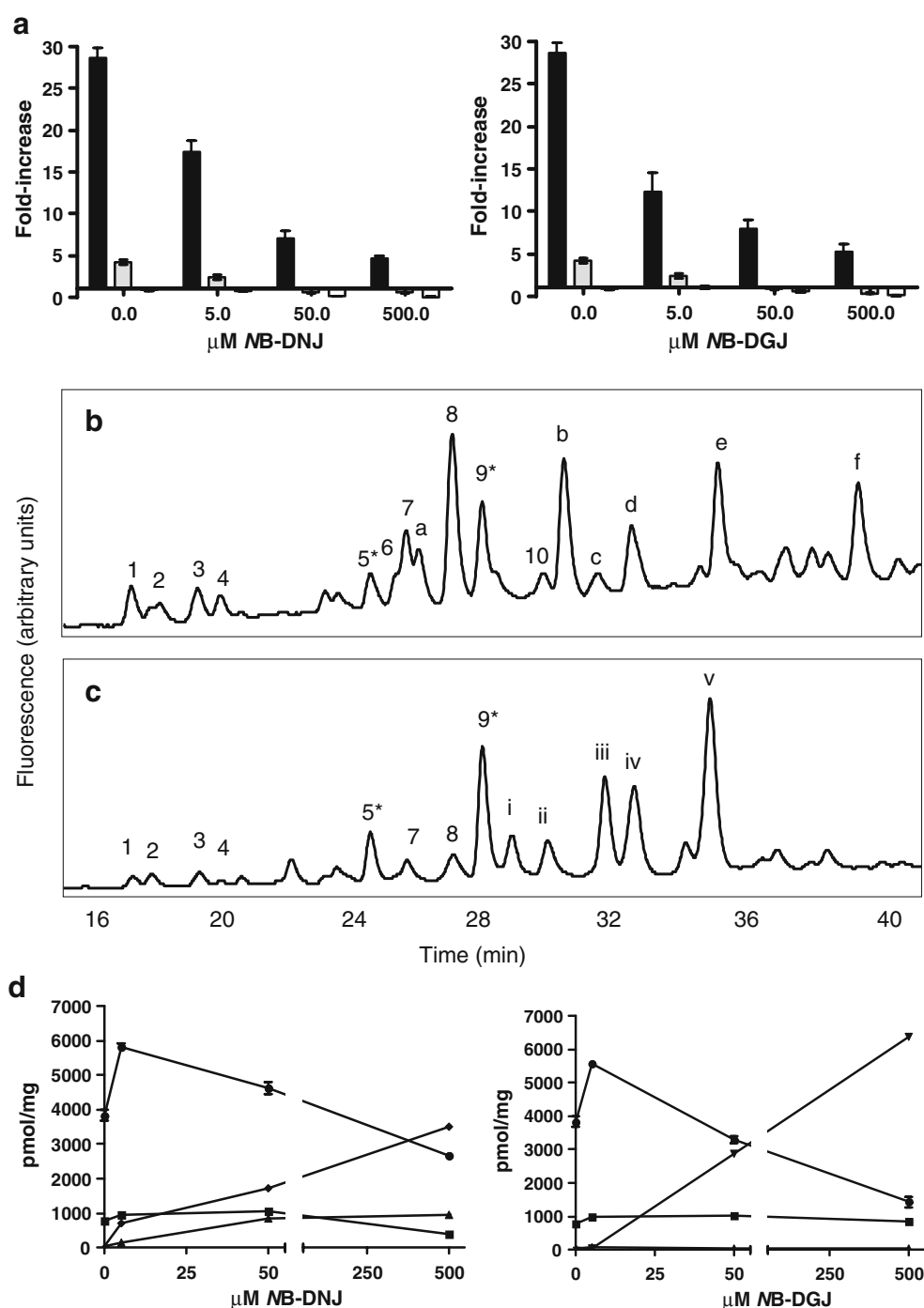
Fig. 3 GSL and OS in hexosaminidase-deficient RAW cells treated with *N*B-DNJ or *N*B-DGJ. RAW cells, grown in the presence of 50 μM SR1, were treated with up to 500 μM *N*B-DNJ or *N*B-DGJ in triplicate for 30 days, before extraction and analysis of the GSL by NP-HPLC. **a** changes in GSL amounts (pmol/mg protein) are shown. *Black bars*, GA2; *grey bars*, GM2 and *white bars*, GMIa. **b** following *N*B-DNJ treatment, OS were extracted and separated by NP-HPLC as described in the "Experimental". The structures of peak numbers 1–10 are shown in Table 2. Peak numbers 5 and 9 (*) are present in control and correspond to oligomannose species Man$_4$GlcNAc$_1$ and Man$_5$GlcNAc$_1$ respectively. All others are GlcNAc-terminating OS. Peaks labelled a–f are additional, glucosylated OS species caused by *N*B-

DNJ treatment; a, Glc$_1$Man$_4$GlcNAc$_1$; b, Glc$_1$Man$_5$GlcNAc$_1$; c, Glc$_3$Man$_4$GlcNAc$_1$; d, Glc$_2$Man$_5$GlcNAc$_1$; e, Glc$_3$Man$_5$GlcNAc$_1$; f, Glc$_3$Man$_7$GlcNAc$_2$, as determined previously [16]. **c** following *N*B-DGJ treatment OS were analysed by NP-HPLC. Peak numbers i–vi are additional, galactose-terminating OS species caused by *N*B-DGJ treatment and the structures are shown in Table 3. **d** total levels, in pmol/mg protein, of GlcNAc-terminating OS, (●); Man$_{4–5}$GlcNAc$_1$, (■); Glc$_1$Man$_5$GlcNAc$_1$, (▲); glucose-terminating OS species following *N*B-DNJ treatment, (♦) and galactose-terminating OS species following *N*B-DGJ treatment (▼), as determined by NP-HPLC separation shown in (**b**) and (**c**). All experiments were performed three times and data are expressed as the mean±SEM

Table 3 OS in β-hexosaminidase deficient RAW cells treated with *N*B-DGJ. Roman numeral peak numbers i–v correspond to those in Fig. 3c. Individual species were collected from the chromatography eluate and characterised further by ß-galactosidase and linkage specific ß-hexosaminidase (pGex17) digestion. The elution values (in glucose units, GU) are shown before and after enzyme treatment. The OS species have the proposed structure indicated. pGeXSTrH17 β-hexosaminidase digestion resulted in more than one product and the relative GU values are shown in order of highest abundancy

No.	GU	GU ß-gal	GU ß-gal & pGex17	Proposed Structure
i	6.11	5.16	4.62, 4.02	+ Galß { Manα6 / Manβ4GlcNAc-2AA, GlcNAcß2Manα3, GlcNAcß4 }
ii	6.45	5.60	4.62, 4.02	+ Galß { GlcNAcß2Manα6 / Manβ4GlcNAc-2AA, GlcNAcß2Manα3, GlcNAcß4 }
iii	6.97	5.16	4.62, 4.02	+ 2 Galß { Manα6 / Manβ4GlcNAc-2AA, GlcNAcß2Manα3, GlcNAcß4 }
iv	7.33	5.60	4.62, 4.02	+ 2 Galß { GlcNAcß2Manα6 / Manβ4GlcNAc-2AA, GlcNAcß2Manα3, GlcNAcß4 }
v	8.13	5.60	4.62, 4.02	+ 3 Galß { GlcNAcß2Manα6 / Manβ4GlcNAc-2AA, GlcNAcß2Manα3, GlcNAcß4 }

above control, but still below those of β-hexosaminidase-inhibited cells.

By contrast, *N*B-DGJ caused a concentration-dependent decline in all cytokine levels in untreated RAW cells (Fig 4d) and cells treated with SR1 (Fig. 4b), and a concentration between 5 µM and 50 µM was required for reducing the cytokine levels to control and thus complete restoration of the cytokine-mediated response. This was the same concentration required for GM2 recovery (data not shown), indicating that the sole contributor to the pathogenesis in the Sandhoff disease cellular model is GM2 ganglioside. No increase in the cytokines was observed following treatment with higher concentrations of *N*B-DGJ, suggesting that the inflammatory response in cells treated with high concentrations of the glucose analogue, *N*B-DNJ, was due to the inhibition of ER α-glucosidases or possibly another activity that has not previously been identified.

Discussion

Substrate reduction therapy (SRT) has striking effects in acute knockout mouse models of GM2 gangliosidoses [7, 8, 24, 25]. Our findings demonstrate the efficacy of SRT drugs that restore the pathogenic GM2 ganglioside storage levels in an imino sugar inhibitor induced *in vitro* cellular model of ß-hexosaminidase deficiency.

Treatment of murine RAW264.7 macrophage-like cells with β-hexosaminidase inhibitor SR1 resulted in accumulation of GM2 and especially GA2 glycolipid. This

Fig. 4 Cytokine levels prior or following treatment with *N*B-DNJ or *N*B-DGJ in chemically induced RAW cells. RAW cells, grown in the presence of 50 μM SR1, were co-treated with up to 500 μM *N*B-DNJ (**a**) or *N*B-DGJ (**b**) in triplicate for 30 days, after which the supernatant was taken for spectrophotometric sandwich ELISA's using TNF-α (■), MIP-1α (●) and TGF-β1 (♦) antibodies. For comparison, RAW cells grown in the absence of SR1 were treated with up to 500 μM *N*B-DNJ (**c**) or *N*B-DGJ (**d**) for 30 days after which ELISA's were performed. The cytokine amount was calculated using a standard, and normalised to cellular protein content. The mean±SEM are shown from three experiments. The levels of MIP-1α are shown in a 1:100 dilution for clarity
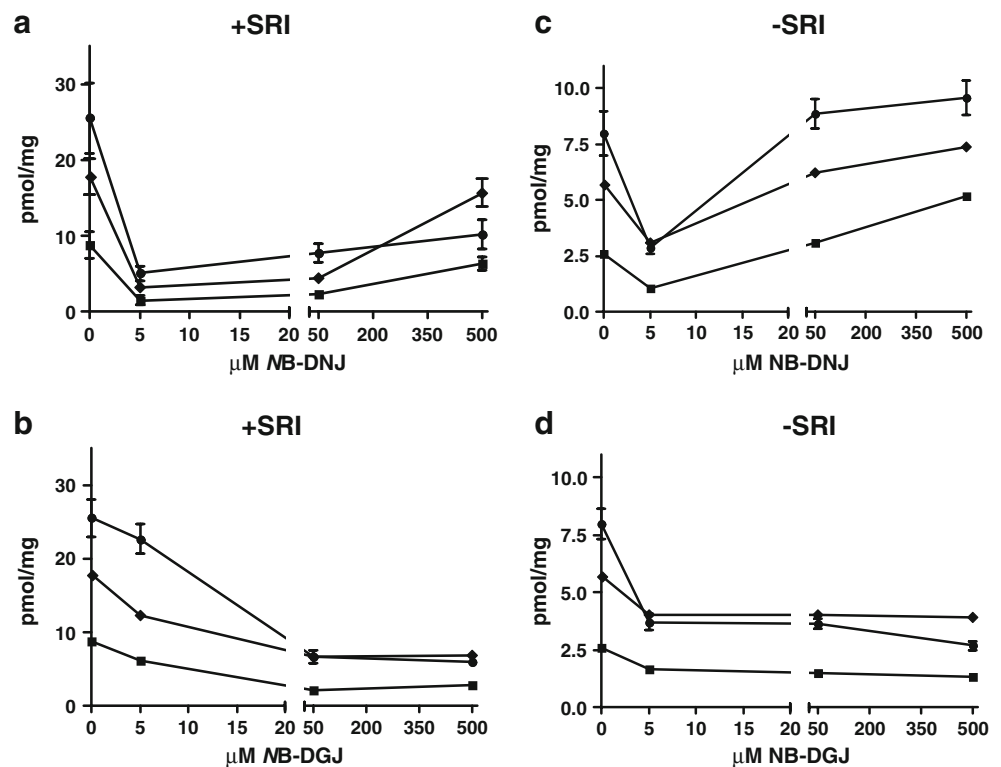
discrepancy in extent of elevation was possibly due to the presence of a mouse-specific sialidase that provides a bypass mechanism by hydrolysing the sialic acid residue from GM2 to form GA2, which in β-hexosaminidase active mice can be degraded by HexB [21, 26]. In neuronal precursor cell cultures from Sandhoff disease and related Tay-Sachs disease model mice, lysosomal sialidase has recently been shown to be active in converting GM2 to GA2 glycolipid [27]. Furthermore, Takahata *et al.* showed by lectin histochemistry, that an α2,3-sialidase is present in the cell line used in this study [28] further explaining the GM2 equilibrium following SR1 treatment.

Besides GM2 and GA2, globoside has been shown to accumulate in Sandhoff patients [29]. This was absent in the cellular model however, and might be due to insufficient globoside biosynthetic potential in RAW264.7 cells.

In addition to GSL, storage of glycoprotein-derived GlcNAc-terminating OS occurred. The major species, a tri-antennary heptasaccharide, has also been found in visceral tissues and is the major storage product in the pancreas of Sandhoff patients [1], indicating the high expression of *N*-acetylglucosaminyl transferase IV in this tissue. Detailed analysis of the N-linked glycoproteins in the mouse leukaemic monocyte macrophage cell line RAW264.7 is in progress and will be required to confirm the preferential biosynthesis of tri-antennary glycans in these cells.

In RAW264.7 cells the storage of glycoconjugates triggered a cytokine-mediated inflammatory response. The prominent role of chemokines MIP-1α and TNF-α in the

GM2 gangliosidoses and related disorders have been well established, and their release is thought to be correlated to GSL storage [4, 5, 30, 31]. TNF-α is known to release nitric oxide (NO) as a consequence of ganglioside storage [32], and thus caspase-dependent apoptosis was prevented [33]. Whether apoptosis was triggered via different mechanisms remains to be elucidated.

Release of TNF-α was accompanied by TGF-β1, thought to antagonise the effects of TNF-α, IL-1, IL-6 and IL-12 produced by microglia and macrophages [22], demonstrating tightly regulated cytokine expression.

In order to elucidate whether the hexosaminidase-inhibited RAW cells remain capable of controlling their cytokine expression via TGF-β1, cells were stimulated with LPS, a toll-like receptor (TLR) agonist. In control RAW cells, LPS induced interferon-γ (IFN-γ) expression, likely via TLRs in a MyD88-dependent manner, which is thought to up-regulate inducible nitric oxide synthase (iNOS) expression [34]. The NO formed has emerged as a potent inhibitor of activated caspases [33], which initiate apoptosis, therefore demonstrating a feedback control loop in the cytokine expression in RAW cells that can then escape programmed cell death.

LPS triggered a differential inflammatory mechanism in hexosaminidase-inhibited RAW cells, thought to be due to the already elevated TNF-α expression. Whereas TGF-β1 remained constant following SR1 and LPS treatment, a dramatic increase in the levels of MIP-1α and especially TNF-α was observed compared to SR1 treatment alone, thus circumventing caspase-dependent apoptosis [33].

Moreover, RANTES was exceptionally pronounced, which is known to rapidly induce expression of MIP-2, MIP-1β, MIP-1α, TNF-α, and IL-6 [35], all of which were elevated following SR1 and LPS co-treatment. In turn, the activated IL-6 has been suggested to exert anti-inflammatory properties by inhibiting TNF-α [36].

The cytokine response following SR1 and LPS treatment, suggests that the TLR signalling pathways are activated, and in particular, the MyD88-dependent cascade (common to all TLRs except TLR3), ultimately resulting in induction of inflammatory mediators such as TNF-α, COX-2 and IL-6 [37]. Whether transcription factor NF-κB, crucial to macrophage activation and initiating transcription of genes encoding TNF-α, iNOS and IL-10 [38], is also activated following LPS treatment, is likely, but has yet to be determined.

Taken together, we propose the presence of a complex, tightly regulated, cytokine-mediated, non-caspase dependent pathway in the hexosaminidase-inhibited cells in response to glycoconjugate storage, providing new insight into the role of lysosomal storage in disease pathology.

Treatment with N-Alkylated imino sugars NB-DNJ and NB-DGJ resulted in normalisation of the inflammatory response at concentrations similar to those required for reduction of the GM2 ganglioside storage burden, but not that of GA2 glycolipid or GlcNAc-terminating OS. Failure of these imino sugars to restore the GA2 level is consistent with recent findings in the Sandhoff mouse model for disease [23].

Both imino sugars raised the storage levels of GlcNAc-terminating OS at low concentrations in SR1-treated cells, and the reason for this is unknown. Higher concentrations however lead to a major decrease; more efficiently by NB-DGJ than by NB-DNJ. The progressive decline caused by the galactose analogue is thought to be due to inhibition of lysosomal β-galactosidase, resulting in capping of the GlcNAc-termini of the major storage products with one or more galactose residue(s), consistent with the pathway for glycoprotein degradation in the lysosome [2]. These galactose-terminating OS are in agreement with those found in the urine of GM1 gangliosidosis (β-gal$^{-/-}$) patients [39], further supporting the ability of NB-DGJ to inhibit lysosomal β-galactosidase, resulting in a GM1 gangliosidosis phenotype in terms of OS storage.

NB-DNJ by contrast, is known to elicit inhibitory activity towards N-glycan processing enzymes ER α-glucosidases I and II [40]. This results in glucosylated oligomannose containing oligosaccharides present on glycoproteins that enter ER quality control pathways before export via the Golgi. If terminally misfolded, the ER-associated degradation (ERAD) pathway translocates glycoproteins to the cytosol, where removal of the oligosaccharide and proteasomal degradation takes place. Therefore, glucosylated OS are observed as a direct consequence of α-glucosidase inhibition by NB-DNJ [11], and ultimately serve as biomarkers for glycoprotein misfolding that may play a role in disease

pathology [16]. It is proposed that NB-DNJ decreased storage of the GlcNAc-terminating OS by either modifying the synthesis of complex glycans to oligomannose-type structures or by increasing the amount of misfolded and degraded glycoprotein. NB-DGJ decreased storage levels more efficiently by inhibiting the lysosomal degradation of galactosylated oligosaccharides, thus masking the GlcNAc-terminating OS as substrates for hexosaminidase.

Intriguingly, low concentrations of NB-DNJ dramatically inhibited the inflammatory response to below control levels, possibly due to novel anti-inflammatory properties, as demonstrated in a mouse model of GM1 gangliosidosis [13]. Caloric restriction caused by appetite suppression [41], which in turn may suppress CNS inflammation [42] cannot be excluded in mouse models for disease. Higher concentrations of NB-DNJ however, appeared to promote rather than suppress the inflammatory response. This observation is possibly due to ER α-glucosidase I and II inhibition, potentially causing an unfolded protein response (UPR) in the ER, resulting in an inflammatory cascade [43]. This remains to be further investigated; however, concentrations that invoke an inflammatory response are in vast excess of that required for the depletion of pathogenic GM2 ganglioside.

NB-DGJ caused complete resolution of the inflammatory response, suggesting that the galactose-terminating OS generated by β-galactosidase inhibition do not contribute to cytokine-mediated pathogenesis. These data also suggest that similar galactosylated oligosaccharides to those stored in GM1 gangliosidosis patients do not play a role in disease pathology. The storage of GM1 ganglioside is therefore implicated in wide-spread neuronal apoptosis and is primarily responsible for the progressive neurodegeneration [44].

In summary, these findings demonstrate the crucial role of GM2 ganglioside in the pathogenesis in an in vitro cellular model. The complete restoration of the GM2 storage burden by N-alkylated imino sugars, and thus the inflammatory response, further support the efficacy of NB-DNJ and NB-DGJ in treating the GM2 gangliosioses.

References

1. Warner, T.G., deKremer, R.D., Sjoberg, E.R., Mock, A.K.: Characterization and analysis of branched-chain N-acetylglucosaminyl oligosaccharides accumulating in Sandhoff disease tissue. Evidence that biantennary bisected oligosaccharide side chains of glycoproteins are abundant substrates for lysosomes. J. Biol. Chem. **260**, 6194–6199 (1985)

2. Winchester, B.: Lysosomal metabolism of glycoproteins. Glycobiology **15**, 1R–15R (2005)

3. Tsuji, D., Kuroki, A., Ishibashi, Y., Itakura, T., Kuwahara, J., Yamanaka, S., Itoh, K.: Specific induction of macrophage inflammatory protein 1-alpha in glial cells of Sandhoff disease model mice

associated with accumulation of N-acetylhexosaminyl glycoconjugates. J. Neurochem. **92**, 1497–1507 (2005)

4. Jeyakumar, M., Thomas, R., Elliot-Smith, E., Smith, D.A., van der Spoel, A.C., d'Azzo, A., Perry, V.H., Butters, T.D., Dwek, R.A., Platt, F.M.: Central nervous system inflammation is a hallmark of pathogenesis in mouse models of GM1 and GM2 gangliosidosis. Brain **126**, 974–987 (2003)

5. Wu, Y.P., Proia, R.L.: Deletion of macrophage-inflammatory protein 1 alpha retards neurodegeneration in Sandhoff disease mice. Proc. Natl. Acad. Sci. U. S. A. **101**, 8425–8430 (2004)

6. Wada, R., Tifft, C.J., Proia, R.L.: Microglial activation precedes acute neurodegeneration in Sandhoff disease and is suppressed by bone marrow transplantation. Proc. Natl. Acad. Sci. U. S. A. **97**, 10954–10959 (2000)

7. Jeyakumar, M., Butters, T.D., Dwek, R.A., Platt, F.M.: Glycosphingolipid lysosomal storage diseases: therapy and pathogenesis. Neuropathol. Appl. Neurobiol. **28**, 343–357 (2002)

8. Platt, F.M., Neises, G.R., Reinkensmeier, G., Townsend, M.J., Perry, V.H., Proia, R.L., Winchester, B., Dwek, R.A., Butters, T.D.: Prevention of lysosomal storage in Tay-Sachs mice treated with N-butyldeoxynojirimycin. Science **276**, 428–431 (1997)

9. Platt, F.M., Neises, G.R., Dwek, R.A., Butters, T.D.: N-butyldeoxynojirimycin is a novel inhibitor of glycolipid biosynthesis. J. Biol. Chem. **269**, 8362–8365 (1994)

10. Platt, F.M., Neises, G.R., Karlsson, G.B., Dwek, R.A., Butters, T.D.: N-butyldeoxygalactonojirimycin inhibits glycolipid biosynthesis but does not affect N-linked oligosaccharide processing. J. Biol. Chem. **269**, 27108–27114 (1994)

11. Mellor, H.R., Neville, D.C., Harvey, D.J., Platt, F.M., Dwek, R.A., Butters, T.D.: Cellular effects of deoxynojirimycin analogues: inhibition of N-linked oligosaccharide processing and generation of free glucosylated oligosaccharides. Biochem. J. **381**, 867–875 (2004)

12. Platt, F.M., Jeyakumar, M., Andersson, U., Heare, T., Dwek, R.A., Butters, T.D.: Substrate reduction therapy in mouse models of the glycosphingolipidoses. Philos. Trans. R. Soc. Lond. B Biol. Sci. **358**, 947–954 (2003)

13. Elliot-Smith, E., Speak, A.O., Lloyd-Evans, E., Smith, D.A., van der Spoel, A.C., Jeyakumar, M., Butters, T.D., Dwek, R.A., d'Azzo, A., Platt, F.M.: Beneficial effects of substrate reduction therapy in a mouse model of GM1 gangliosidosis. Mol. Genet. Metab. **94**, 204–211 (2008)

14. Rountree, J.S.S., Butters, T.D., Wormald, M.R., Dwek, R.A., Asano, N., Ikeda, K., Evinson, E.L., Nash, R.J., Fleet, G.W.J.: Efficient synthesis from D-lyxonolactone of 2-acetamido-1, 4-imino-1, 2, 4-trideoxy-L-arabinitol LABNAc, a potent pyrrolidine inhibitor of hexosaminidases. Tetrahedron Lett. **48**, 4287–4291 (2007)

15. Neville, D.C., Coquard, V., Priestman, D.A., Te Vruchte, D.J., Sillence, D.J., Dwek, R.A., Platt, F.M., Butters, T.D.: Analysis of fluorescently labeled glycosphingolipid-derived oligosaccharides following ceramide glycanase digestion and anthranilic acid labeling. Anal. Biochem. **331**, 275–282 (2004)

16. Alonzi, D.S., Neville, D.C., Lachmann, R.H., Dwek, R.A., Butters, T.D.: Glucosylated free oligosaccharides are biomarkers of endoplasmic-reticulum alpha-glucosidase inhibition. Biochem. J. **409**, 571–580 (2008)

17. Mellor, H.R., Neville, D.C., Harvey, D.J., Platt, F.M., Dwek, R.A., Butters, T.D.: Cellular effects of deoxynojirimycin analogues: uptake, retention and inhibition of glycosphingolipid biosynthesis. Biochem. J. **381**, 861–866 (2004)

18. Harvey, D.J., Dwek, R.A., Rudd, P.M. Determining the structure of glycan moieties by mass spectrometry. Curr. Protoc. Protein Sci. **Chapter 12**, Unit 12 17 (2006)

19. Clarke, V.A., Platt, N., Butters, T.D.: Cloning and expression of the beta-N-acetylglucosaminidase gene from Streptococcus pneumoniae. Generation of truncated enzymes with modified aglycon specificity. J. Biol. Chem. **270**, 8805–8814 (1995)

20. Rountree, J.S.S., Butters, T.D., Wormald, M.R., Boomkamp, S.D., Dwek, R.A., Asano, N., Ikeda, K., Evinson, E.L., Nash, R.J., Fleet, G.W.J.: Design, synthesis, and biological evaluation of enantiomeric beta-N-acetylhexosaminidase inhibitors LABNAc and DABNAc as potential agents against Tay-Sachs and Sandhoff disease. ChemMedChem **4**, 378–392 (2009)

21. Sango, K., Yamanaka, S., Hoffmann, A., Okuda, Y., Grinberg, A., Westphal, H., McDonald, M.P., Crawley, J.N., Sandhoff, K., Suzuki, K., Proia, R.L.: Mouse models of Tay-Sachs and Sandhoff diseases differ in neurologic phenotype and ganglioside metabolism. Nat. Genet. **11**, 170–176 (1995)

22. Martiney, J.A., Cuff, C., Litwak, M., Berman, J., Brosnan, C.F.: Cytokine-induced inflammation in the central nervous system revisited. Neurochem. Res. **23**, 349–359 (1998)

23. Baek, R.C., Kasperzyk, J.L., Platt, F.M., Seyfried, T.N.: N-butyldeoxygalactonojirimycin reduces brain ganglioside and GM2 content in neonatal Sandhoff disease mice. Neurochem. Int. **52**, 1125–1133 (2008)

24. Jeyakumar, M., Butters, T.D., Cortina-Borja, M., Hunnam, V., Proia, R.L., Perry, V.H., Dwek, R.A., Platt, F.M.: Delayed symptom onset and increased life expectancy in Sandhoff disease mice treated with N-butyldeoxynojirimycin. Proc. Natl. Acad. Sci. U. S. A. **96**, 6388–6393 (1999)

25. Andersson, U., Smith, D., Jeyakumar, M., Butters, T.D., Borja, M.C., Dwek, R.A., Platt, F.M.: Improved outcome of N-butyldeoxygalactonojirimycin-mediated substrate reduction therapy in a mouse model of Sandhoff disease. Neurobiol. Dis. **16**, 506–515 (2004)

26. Phaneuf, D., Wakamatsu, N., Huang, J.Q., Borowski, A., Peterson, A.C., Fortunato, S.R., Ritter, G., Igdoura, S.A., Morales, C.R., Benoit, G., Akerman, B.R., Leclerc, D., Hanai, N., Marth, J.D., Trasler, J.M., Gravel, R.A.: Dramatically different phenotypes in mouse models of human Tay-Sachs and Sandhoff diseases. Hum. Mol. Genet. **5**, 1–14 (1996)

27. Martino, S., di Girolamo, I., Cavazzin, C., Tiribuzi, R., Galli, R., Rivaroli, A., Valsecchi, M., Sandhoff, K., Sonnino, S., Vescovi, A., Gritti, A., Orlacchio, A.: Neural precursor cell cultures from GM2 gangliosidosis animal models recapitulate the biochemical and molecular hallmarks of the brain pathology. J. Neurochem. **109**, 135–147 (2009)

28. Takahata, M., Iwasaki, N., Nakagawa, H., Abe, Y., Watanabe, T., Ito, M., Majima, T., Minami, A.: Sialylation of cell surface glycoconjugates is essential for osteoclastogenesis. Bone **41**, 77–86 (2007)

29. Tatematsu, M., Imaida, K., Ito, N., Togari, H., Suzuki, Y., Ogiu, T.: Sandhoff disease. Acta. Pathol. Jpn. **31**, 503–512 (1981)

30. van Breemen, M.J., de Fost, M., Voerman, J.S., Laman, J.D., Boot, R.G., Maas, M., Hollak, C.E., Aerts, J.M., Rezaee, F.: Increased plasma macrophage inflammatory protein (MIP)-1alpha and MIP-1beta levels in type 1 Gaucher disease. Biochim. Biophys. Acta **1772**, 788–796 (2007)

31. Mizutani, K., Oka, N., Akiguchi, I., Satoi, H., Kawasaki, T., Kaji, R., Kimura, J.: Enhancement of TNF-alpha production by ganglioside GM2 in human mononuclear cell culture. NeuroReport **10**, 703–706 (1999)

32. Pyo, H., Joe, E., Jung, S., Lee, S.H., Jou, I.: Gangliosides activate cultured rat brain microglia. J. Biol. Chem. **274**, 34584–34589 (1999)

33. Kim, Y.M., Talanian, R.V., Billiar, T.R.: Nitric oxide inhibits apoptosis by preventing increases in caspase-3-like activity via two distinct mechanisms. J. Biol. Chem. **272**, 31138–31148 (1997)

34. Kim, Y.M., Talanian, R.V., Li, J., Billiar, T.R.: Nitric oxide prevents IL-1beta and IFN-gamma-inducing factor (IL-18) release from macrophages by inhibiting caspase-1 (IL-1beta-converting enzyme). J. Immunol. **161**, 4122–4128 (1998)

35. Fischer, F.R., Luo, Y., Luo, M., Santambrogio, L., Dorf, M.E.: RANTES-induced chemokine cascade in dendritic cells. J. Immunol. **167**, 1637–1643 (2001)

36. Di Santo, E., Alonzi, T., Poli, V., Fattori, E., Toniatti, C., Sironi, M., Ricciardi-Castagnoli, P., Ghezzi, P.: Differential effects of IL-6 on systemic and central production of TNF: a study with IL-6-deficient mice. Cytokine **9**, 300–306 (1997)

37. Akira, S., Takeda, K.: Toll-like receptor signalling. Nat. Rev. Immunol. **4**, 499–511 (2004)

38. Muller, J.M., Ziegler-Heitbrock, H.W., Baeuerle, P.A.: Nuclear factor kappa B, a mediator of lipopolysaccharide effects. Immunobiology **187**, 233–256 (1993)

39. Klein, A., Lebreton, A., Lemoine, J., Perini, J.M., Roussel, P., Michalski, J.C.: Identification of urinary oligosaccharides by matrix-assisted laser desorption ionization time-of-flight mass spectrometry. Clin. Chem. **44**, 2422–2428 (1998)

40. Dwek, R.A., Butters, T.D., Platt, F.M., Zitzmann, N.: Targeting glycosylation as a therapeutic approach. Nat. Rev. Drug Discov. **1**, 65–75 (2002)

41. Priestman, D.A., van der Spoel, A.C., Butters, T.D., Dwek, R.A., Platt, F.M.: N-butyldeoxynojirimycin causes weight loss as a result of appetite suppression in lean and obese mice. Diabetes Obes. Metab. **10**, 159–166 (2008)

42. Denny, C.A., Kasperzyk, J.L., Gorham, K.N., Bronson, R.T., Seyfried, T.N.: Influence of caloric restriction on motor behavior, longevity, and brain lipid composition in Sandhoff disease mice. J. Neurosci. Res. **83**, 1028–1038 (2006)

43. Pahl, H.L., Baeuerle, P.A.: A novel signal transduction pathway from the endoplasmic reticulum to the nucleus is mediated by transcription factor NF-kappa B. EMBO J. **14**, 2580–2588 (1995)

44. Sano, R., Tessitore, A., Ingrassia, A., d'Azzo, A.: Chemokine-induced recruitment of genetically modified bone marrow cells into the CNS of GM1-gangliosidosis mice corrects neuronal pathology. Blood **106**, 2259–2268 (2005)